

AN INVESTIGATION OF HANDLEY PAGE JETSTREAM HANDLING DURING LANDING - NONLINEAR ASPECTS

G. Mullen, F. Marodon
Cranfield University

Abstract

Handley Page Jetstream G-NFLC is heavily used as an airborne laboratory platform. In some circumstances, the aeroplane may be prone to pilot involved oscillations in pitch during the flare. In a previous study, linear mathematical models of the short period dynamics (estimated from flight data) were assessed against the Gibson dropback and phase rate criteria. In both cases, the aircraft response was judged to be marginally satisfactory. In this investigation, the (nonlinear) effect of inceptor dead band is taken into account. The stability of the combined linear and nonlinear elements is assessed using the Nyquist criterion, where it is shown that a pilot involved oscillation is now a distinct possibility, particularly at aft centre of gravity locations.

Nomenclature

c.g.	Centre of gravity
\bar{c}	Standard mean chord
DB	Dropback
$F_p(s)$	Pilot model transfer function
k	Numerator gain in η/P_η transfer function
k_q	Numerator gain in q/η transfer function
m_q	Pitching moment due to pitch rate (concise derivative)
m_w	Pitching moment due to normal velocity (concise derivative)

m_η	Pitching moment due to elevator deflection (concise derivative)
N	Describing function
NFLC	The National Flying Laboratory Centre
PIO	Pilot involved oscillation
P_η	Longitudinal stick force
q	Pitch rate perturbation
q_{\max}	Peak pitch rate perturbation
q_{ss}	Steady state pitch rate perturbation
s	Laplace operator
$T_{\theta 2}$	Numerator zero in elevator to pitch rate transfer function
U_e	Trim airspeed
w	Normal velocity perturbation
z_q	Normal force due to pitch rate (concise derivative)
z_w	Normal force due to normal velocity (concise derivative)
z_η	Normal force due to elevator deflection (concise derivative)
η	Elevator deflection perturbation
ζ	Damping ratio, η/P_η transfer function
ζ_s	Short period damping ratio
ω	Undamped natural frequency, η/P_η transfer function
ω_s	Short period undamped natural frequency
\dot{x}	dx/dt

1 Introduction

Handley Page Jetstream 100 G-NFLC (Fig. 1), operated by the National Flying Laboratory Centre (NFLC) at Cranfield University College of Aeronautics fulfills a variety of teaching and research tasks.

Such a wide range of activities is made possible by a flexible in-house digital instrumentation and display system. Sensors located around the aircraft measure a variety of signals which are then converted in the signal conditioning unit and digital system prior to presentation on the observers display panels.

In-house software [1] is available for post-flight data processing, and allows the user to convert the measurements into various forms suitable for use with proprietary packages, e.g. *MATLAB*TM.

Unfortunately, the handling characteristics do not inspire the same enthusiastic comments as the instrumentation system. In some circumstances the aeroplane may be prone to pilot involved oscillations (PIO) in pitch during the flare. One such event is shown in Fig. 2.

The aircraft was loaded to within 4% of the aft centre of gravity (c.g.) limit and the trial flown on a day with a strong gusty wind, with some crosswind component. The crew consisted of two qualified test pilots of similar overall experience, the aircraft commander (pilot A), had accumulated approximately 1600 hours and 2100 landings on the test aircraft over the preceding 6 years in a wide range of weather conditions. The “co-pilot” had not flown a Jetstream before. A total of eight circuits were made. During the first six circuits pilot A made a number of landings with a variety of lateral and vertical offsets designed to further elevate pilot gain. Whilst the workload was noticeably higher during these approaches no uncontrolled oscillations were encountered.

When pilot B attempted to land the aircraft on the seventh circuit a PIO developed during the flare. It can be seen on the data recording, starting at time 85 seconds and persisting until time 100 seconds, that the behaviour of the aircraft has a different characteristic; this is

most easily seen on pitch attitude, which appears to be oscillating at a constant frequency. Either side of this time window, the pitch attitude has a more random appearance. Within this 15 second period, the elevator deflection also has a distinctly different appearance.

During the approach, before time 85 seconds on the recording, the aircraft was repeatedly upset by the turbulence and pilot B responded with corrections. As the aircraft descended through approximately 50 ft (time 85 seconds) a PIO started. From the flight deck viewpoint the nose of the aircraft rose and fell between two extremes, at the nose down peak the attitude was unacceptable for landing as a touchdown on the nosewheel would have resulted, while at the nose up peak the aircraft was no longer closing with the runway in the normal manner, giving the impression of climbing away with reducing airspeed - also unacceptable. The pilot attempted to recover the aircraft from each unacceptable attitude extreme but the response to his corrections led to the aircraft overshooting the desired attitude. The absolute height during the PIO was not recorded by the data acquisition system but was estimated to cycle between 5 ft. and 25 ft., and the close proximity of the runway kept pilot gain high. When the airspeed had decayed to some 12 kt below the scheduled threshold speed a go-around was initiated - time 100 seconds on the data recording. Once the landing attempt was abandoned the oscillation died out. Thereafter the character of pilot activity returned to that observed before the PIO. Pilot B made a second landing attempt and although a PIO developed during the flare a safe landing was made on this occasion.

The most likely causes of the tendency towards PIO's are a deterioration in the short period dynamics at aft c.g. locations and adverse longitudinal stick force characteristics - a combination of frequency, damping and dead band effects.

In a previous study [2] the above linear components were estimated from flight data and the susceptibility to PIOs evaluated against the

Gibson dropback [3] and phase rate [4] boundaries. There was no evidence of a tendency towards PIOs, although the dynamics were judged to be marginal:- in terms of dropback, the short period response was very close to the boundary between “satisfactory” and “sluggish”; in terms of phase rate, it was close to the border between “no PIO” and “moderate PIO”.

In this paper, the (nonlinear) effect of inceptor dead band is included in the analysis. The general structure is as follows. In Section 2 the flight test experiments and conditions are briefly described, while Section 3 presents a summary of the linear analysis. Nonlinear aspects, and their effect on the susceptibility to PIOs are considered in Section 4. Some conclusions are offered in Section 5.

Before proceeding further, it must be emphasised that the NFLC operates a prototype Handley Page Jetstream and *not* a production BAE Systems Jetstream. In handling terms there are several critical differences between the two types; therefore the conclusions drawn in this study relate *exclusively* to the aircraft operated by the NFLC.

2 Flight Tests

Although the above mentioned test was successful in that a PIO was observed and recorded, it did not provide any hard information about those aircraft characteristics which may be at the root cause of the problem. Consequently, a set of flight tests were conducted with the specific aim of identifying and quantifying the open loop longitudinal dynamics.

The data presented in the remainder of this paper arise from a single dedicated flight with the aircraft loaded at representative mid and aft c.g. locations:- 23.5 % and 31.8 % of the standard mean chord (\bar{c}) respectively. Prior to the application of the test inputs, the aircraft was trimmed in the landing configuration (landing flap selected, landing gear down) at an airspeed of between 115 *kt* and 120 *kt*.

Two types of excitation were applied at each loading configuration. Assuming firstly that the dynamics are linear, a *transient* (pulse type) input was used, the aim being to excite the short period dynamics.

However, recognising that there are nonlinear components, the aircraft was also subjected to a *sinusoidal* input of varying frequencies and amplitudes.

3 A Summary of the Linear Analysis

This Section summarises the signal processing and parameter identification techniques used in the linear analysis. Parametric models of the short period response are presented, and the effect of c.g. location and stick force characteristics are discussed. The reader is directed to [2] for a detailed description.

3.1 Signal Processing

Prior to identifying linear models from the flight data, the following steps were required:- remove all steady state offsets, ensure that a consistent set of units is used, remove measurement system delays, check the signal coherence and filter as required. All calculations were carried out using the *MATLAB*TM signal processing toolbox [5].

3.1 Elevator Deflection to Pitch Rate Response

The processed signals are used to generate state-space models of the short period motion [6]:

$$\begin{bmatrix} \dot{w} \\ \dot{q} \end{bmatrix} = \begin{bmatrix} z_w & z_q \\ m_w & m_q \end{bmatrix} \begin{bmatrix} w \\ q \end{bmatrix} + \begin{bmatrix} z_\eta \\ m_\eta \end{bmatrix} \eta \quad (1)$$

where η is the elevator perturbation; w and q the vertical velocity and pitch rate perturbations respectively. The numerical values of the elements in equation (1) were estimated for both data sets using a simple regression analysis [7].

The derivatives thus estimated at a c.g. position of 23.5 % \bar{c} are:

$$\begin{bmatrix} \dot{w} \\ \dot{q} \end{bmatrix} = \begin{bmatrix} -0.893 & 59.5126 \\ -0.0565 & -1.2733 \end{bmatrix} \begin{bmatrix} w \\ q \end{bmatrix} + \begin{bmatrix} 26.4456 \\ -1.2733 \end{bmatrix} \eta \quad (2)$$

With the c.g. located at $31.8\% \bar{c}$ the corresponding derivatives are:

$$\begin{bmatrix} \dot{w} \\ \dot{q} \end{bmatrix} = \begin{bmatrix} -0.9523 & 56.5061 \\ -0.029 & -1.1632 \end{bmatrix} \begin{bmatrix} w \\ q \end{bmatrix} + \begin{bmatrix} 20.7793 \\ -5.1707 \end{bmatrix} \eta \quad (3)$$

From a knowledge of the physics of the problem, and a comparison with simulated values, all derivative estimates except z_η are considered to be reasonable. However, the error in the latter has only a minor effect on the handling qualities analysis - see [2] for more details.

From a handling qualities viewpoint, it is convenient to convert the pitch rate state equations (2) and (3) to the transfer function form:-

$$\frac{q(s)}{\eta(s)} = \frac{m_\eta(s - z_w)}{[s^2 - (m_q + z_w)s + (m_q z_w - m_w U_e)]} = \frac{k_q(s + 1/T_{\theta 2})}{s^2 + 2\zeta_s \omega_s s + \omega_s^2} \quad (4)$$

$$\frac{q(s)}{\eta(s)} = \frac{-4.9769(s + 1.193)}{(s^2 + 2.166s + 4.497)} \text{rad/sec/rad}, \quad 23.5\% \bar{c} \quad (5)$$

$$\frac{q(s)}{\eta(s)} = \frac{-5.1707(s + 1.069)}{(s^2 + 2.116s + 2.7439)} \text{rad/sec/rad}, \quad 31.8\% \bar{c} \quad (6)$$

Using the measured elevator perturbations as inputs to the above transfer functions, the maximum difference between the predicted and actual pitch rates in the time domain is 8 % of the peak value of the actual pitch rate at 23.5 % \bar{c} ; the corresponding figure at 31.8 % \bar{c} is 5 %. From Fig. 3 it may be seen that the pitch rates predicted by equations (5) and (6) agree closely with the measured perturbations.

3.2 Longitudinal Stick Force to Elevator Deflection Response

Fig. 4 shows a frequency domain estimate of the longitudinal stick force (P_η) to elevator deflection at a c.g. location of $23.5\% \bar{c}$; a similar result is obtained at $31.8\% \bar{c}$. Note that the steady state phase should be -180 deg ; this is the case but the phase has been corrected to read 0 deg at low frequency for the sake of clarity. The modified phase appears to approach

a high frequency limit of -180 deg , thus suggesting a transfer function of the form:-

$$\frac{\eta(s)}{P_\eta(s)} = \frac{k}{s^2 + 2\zeta_s \omega_s s + \omega_s^2} \quad (7)$$

Consequently, consideration of the gain and phase curves suggests the numerical values:-

$$\frac{\eta(s)}{P_\eta(s)} = \frac{-0.1}{s^2 + 6s + 100} \text{rad/N} \quad (8)$$

The above transfer function model provides a reasonable match to the phase of the raw data, Fig. 4. Using the measured P_η signal as an input to equation (8), the maximum difference between the predicted and actual elevator deflections in the time domain is 25 % of the peak value of the actual deflections.

3.3 Longitudinal Stick Force to Pitch Rate Response

Using equations (4) and (7), the longitudinal stick force to pitch rate transfer function is:-

$$\frac{q(s)}{P_\eta(s)} = \frac{k k_q (s + 1/T_{\theta 2})}{(s^2 + 2\zeta_s \omega_s s + \omega_s^2)(s^2 + 2\zeta_s \omega_s s + \omega_s^2)} \quad (9)$$

Substituting the numerical values derived previously, the transfer functions for each configuration are:-

$$\frac{q(s)}{P_\eta(s)} = \frac{0.498(s + 1.193)}{(s^2 + 6s + 100)(s^2 + 2.166s + 4.497)} \text{rad/sec/N}, \quad 23.5\% \bar{c} \quad (10)$$

$$\frac{q(s)}{P_\eta(s)} = \frac{0.517(s + 1.069)}{(s^2 + 6s + 100)(s^2 + 2.116s + 2.7439)} \text{rad/sec/N}, \quad 31.8\% \bar{c} \quad (11)$$

With the measured P_η perturbations as inputs to the above transfer functions, the maximum difference between the predicted and actual pitch rates in the time domain is 32 % of the peak value of the actual pitch rate at $23.5\% \bar{c}$; the corresponding figure at $31.8\% \bar{c}$ is 26 %.

Consideration of the results thus far suggests that the greatest source of error is due

to the estimation of the elevator force to elevator deflection characteristics.

3.4 Applying the Dropback Criterion

Considering first the $q(s)/\eta(s)$ response, the numerical values required to plot the pitch axis dynamics on the dropback diagram can be extracted from the transfer functions (5) and (6) - a step response test gives q_{\max}/q_{ss} , substitution of ω_s , ζ_s and $T_{\theta 2}$ into:-

$$\frac{DB}{q_{ss}} = T_{\theta 2} - \frac{2\zeta_s}{\omega_s} \text{ (sec)} \quad (12)$$

gives DB/q_{ss} (the dropback). The results are shown in Table 1 and Fig. 5.

Table 1: Dropback parameters

c. g. (% \bar{c})	ω_s (rad/sec)	ζ_s	$T_{\theta 2}$ (sec)	DB/q_{ss} (sec)	q_{\max}/q_{ss} (sec)
23.5	2.1207	0.5108	0.838	0.3565	1.581
31.8	1.6565	0.6386	0.936	0.165	1.328

In both cases, the aircraft response falls inside the satisfactory region, although as the c.g. moves aft, there is a 54% reduction in DB/q_{ss} . Since the airframe short period dynamics are adequately described by the standard second order model it is possible to trace the reduction in dropback directly to the derivatives governing the short period response.

Considering equation (12) and Table 1, it may be seen that $T_{\theta 2}$ increases by 12 % as the c.g. moves aft (in theory it should be invariant); in contrast the factor $2\zeta_s/\omega_s$ increases by 60 % and therefore dominates the reduction in dropback. The movement in $2\zeta_s/\omega_s$ is comprised of a 22 % reduction in ω_s and a 25 % increase in ζ_s ; these in turn can be traced to changes in the appropriate aerodynamic derivatives. From equation (4), the short period natural frequency is:

$$\omega_s = \sqrt{m_q z_w - m_w U_e} \quad (13)$$

Substituting the numerical values at each flight condition reveals that the factor $m_q z_w$ reduces by approximately 3 % as the c.g. moves aft; conversely the factor $m_w U_e$ reduces by 51 %. Since the trim airspeed in each case is similar the reduction in $m_w U_e$ must be due to a decrease in m_w ; consideration of equations (2) and (3) shows this to be the case. Since m_w is strongly related to the static margin [6], the reduction in ω_s can be attributed to a reduced static margin as the c.g. moves aft.

From Table 1, the damping $2\zeta_s \omega_s$ is roughly constant between both configurations. However the damping ratio:

$$\zeta_s = \frac{-(m_q + z_w)}{2\omega_s} \quad (14)$$

increases by 25%. Since the factor $(m_q + z_w)$ varies by only 2% between the two configurations, the increase in ζ_s must come largely from the reduction in ω_s and hence the static margin.

The longitudinal stick force to pitch rate response can be treated in a similar manner. By producing a second order match to transfer functions (10) and (11), the resulting dynamics can be assessed against the dropback criterion.

The results are shown in Fig. 5. With the longitudinal stick forces included, the dropback at 23.5% \bar{c} reduces by only 10%. At 31.8% \bar{c} , there is an 87% reduction. The aft c.g. case is particularly interesting, since the response is now very close to the boundary between dropback and overshoot

3.5 Applying the Phase Rate Criterion

The phase rate criterion is concerned with the attitude phase slope in the region of the -180 deg lag frequency. However, the relationships developed thus far - transfer functions (5), (6) and (10), (11) - have been concerned with pitch rate; consequently for the remainder of this analysis the above transfer functions are multiplied by a $1/s$ term.

Firstly elevator deflection to pitch rate. Due to the sign convention, (positive elevator deflection causes a negative pitch rate) the steady state phase associated with transfer functions (5) and (6) is -180 deg . Adjusting this to 0 deg and multiplying by $1/s$ gives a low frequency phase of -90 deg and a high frequency asymptote of -180 deg . The elevator deflection to pitch attitude dynamics are therefore characterised by zero phase rate and a high neutral stability frequency, Fig 6. In other words there is no PIO tendency; reasonable changes in the location of the c.g. will not alter the situation since the phase rate will always be zero and the -180 deg lag frequency will remain high.

This contrasts with the results of Section 3.4 which showed a 54 % reduction in dropback as the c.g. moved aft. However, in both cases the dropback was positive, thus implying a satisfactory response. Viewed in that light, both phase rate and dropback criteria are broadly in agreement.

Using the modified transfer functions (10) and (11), the phase rate at $23.5 \% \bar{c}$ is approximately 84 deg/Hz with a neutral stability frequency of 0.7 Hz ; the corresponding values at $31.8 \% \bar{c}$ are 80 deg/Hz and 0.67 Hz . From Fig. 6, this places the pitch response just under the boundary between “no PIO” and “moderate PIO”.

Therefore although the criterion does not predict the occurrence of a PIO for the Jetstream, the stiffness and damping between longitudinal stick force and elevator deflection clearly have a negative impact (as per pilot opinion) on the overall aircraft response, since the dynamics are now far removed from the “low order” region occupied by the bare airframe short period.

3.6 Summary of the Linear Analysis

- According to both criteria, the aircraft response is marginally satisfactory.

- As the c.g. moves aft, the dropback associated with the bare airframe short period dynamics reduces.
- This is due to a reduction in the short period natural frequency which is due to a decrease in the derivative m_w , and hence the static margin.
- The effect is broadly in agreement with pilot comment which states that the aircraft response becomes more sluggish as the c.g. moves aft.
- The stiffness and damping between longitudinal stick force and elevator deflection cause a large reduction in dropback (at $31.8\% \bar{c}$) and a substantial increase in phase rate (both c.g. locations).

4 Nonlinear Aspects

The following paragraphs represent a summary of the nonlinear work carried out by the second author during his MSc studies.

4.1 Dead Band

Following discussions with the Chief Test Pilot, it was decided that the dominant nonlinearity in the elevator control circuit is a force dead band; i.e. there is a threshold stick force below which no elevator deflection occurs. The size of this dead band is approximately $\pm 13 \text{ N}$ (3 lbf). Beyond this, it is assumed that equation (8) holds.

The dead band may be modelled using the describing function N [8]:-

$$N = \frac{\eta}{P_\eta} \equiv \begin{cases} \frac{1}{\pi}(\pi - 2\beta - \sin 2\beta), & P_\eta > d \\ 0, & 0 \leq P_\eta \leq d \end{cases} \quad (15)$$

where d is the size of the dead band, and

$$\beta = \sin^{-1}\left(\frac{d}{P_\eta}\right) \quad (16)$$

The slope, k , has been accounted for in equation (8), and is therefore equal to unity here.

A dead band element influences only the gain. This was confirmed by the sinusoidal input tests described in Section 2. Two force

amplitude levels were used to excite the aircraft; one just above the threshold, the other roughly 3 times the dead band. Comparing the stick force to pitch attitude response in each case, it was found that the low force input attenuated the low frequency gain, but that both force levels produced the same phase characteristics. Similar behaviour was observed on the Jetstream simulation model, thus suggesting that dead band is indeed the dominant nonlinearity.

4.2 Stability Analysis

In attempting to determine the effect of the dead band on the overall stability, it was decided to use a rigorous mathematical approach, rather than attempt to adapt the techniques currently used to evaluate linear systems, e.g. those described in Section 3.

One method which is familiar to the control community is the Nyquist criterion. As will be shown below, this lends itself very well to the approximate analysis of systems containing a combination of linear and nonlinear components [8].

Consider the closed loop system shown in Fig. 7, where N represents the describing function, and $F(s)$ the linear element(s). For a sinusoidal input, the closed loop transfer function will be:-

$$G = \frac{NF(s)}{1 + NF(s)} \quad (17)$$

The stability of the closed loop system may be assessed using the Nyquist stability criterion:-

$$1 + NF(s) = 0 \quad (18)$$

or more usually:-

$$F(s) = -\frac{1}{N} \quad (19)$$

Therefore the stability of the closed loop system can be assessed by plotting $F(s)$ and $-1/N$ together on the Nyquist diagram.

4.3 Pilot Model

A variety of models are currently used to describe the behaviour of the human pilot. One of the simplest consists of a gain and lag [9]:-

$$F_p(s) = \frac{1529}{0.2s+1} N/\text{rad} \quad (20)$$

The complete open loop dynamics are therefore a series combination of the linear stick force to attitude dynamics as described by the integral of equations (10) or (11), the dead band, and the pilot model.

4.4 Results

Considering the 23.5 % \bar{c} case, Fig. 8, the loci intersect at $-1/N = -1.155$ and a frequency of 2.75 rad/sec (0.44 Hz). This value of $-1/N$ corresponds to an input force of 128 N (29 lbf). Consequently, there is a possible limit cycle occurrence at the above amplitude and frequency. To put this in perspective, the Chief Test Pilot estimated that the maximum level of force typically applied is around 40 lbf, and that only for short periods during trim changes caused by the flaps or landing gear.

At the aft c.g. location of 31.8 % \bar{c} , the forcing amplitude and frequency fall within more reasonable bounds. From Fig. 9, the curves intersect at $-1/N = -1.3945$ and a frequency of 2.39 rad/sec (0.38 Hz). This represents a force amplitude of only 59 N (13 lbf). While the frequency is not radically different from the mid c.g. case, the input force is very close to that used to manoeuvre the aircraft under "normal" conditions -10 lbf.

Consequently, problems are more likely to occur when the aircraft is loaded to aft c.g. locations

5 Conclusions

- The linear dynamics are marginal, but the aircraft is not PIO prone.
- Including the dead band nonlinearity suggests that PIOs are a distinct possibility, particularly at aft c.g. locations.

References

- [1] Stevens J. *Data recording and POSTFLT analysis software*, V2.00, Cranfield Aerospace Ltd., 1995.
- [2] Mullen G. An investigation of Handley Page Jetstream handling during landing, *submitted to The Aeronautical Journal*.
- [3] Gibson J. Piloted handling qualities design criteria for high order flight control systems, *AGARD CP-333*, 1982.
- [4] Gibson J. Handling qualities for unstable combat aircraft, *ICAS-86-5.3.4*, 1986.
- [5] *MATLAB™ Signal processing toolbox*, V3.0b, 1994.
- [6] Cook M.V. *Flight dynamics principles*, 1st edition, Arnold, 1997.
- [7] Klein V. *Parameter identification applied to aircraft*, Cranfield Institute of Technology, PhD thesis, 1973.
- [8] Raven F. *Automatic control engineering*, 2nd edition, McGraw-Hill, 1968.
- [9] Anderson M. and Page R. Pilot induced oscillations involving multiple nonlinearities, *Journal of Guidance, Control and Dynamics*, Vol. 21, No. 5, 1998.



Figure 1. Cranfield University Jetstream and Bulldog.

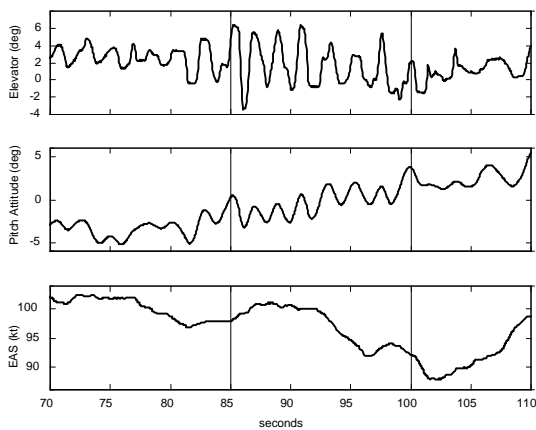


Figure 2. Jetstream PIO during the flare.

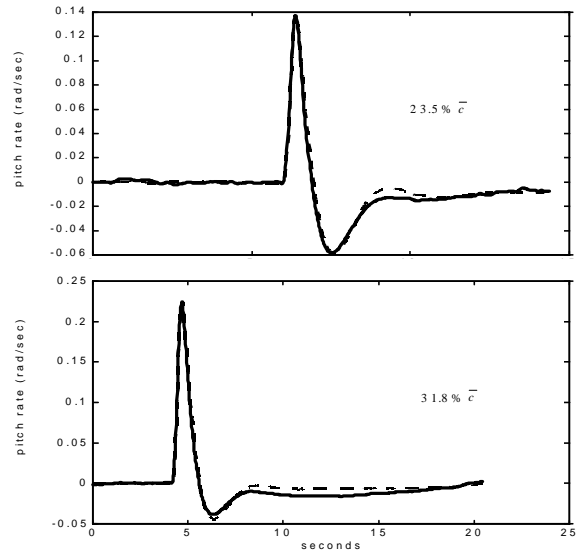


Figure 3. Estimated (--) and actual (-) pitch rate perturbations.

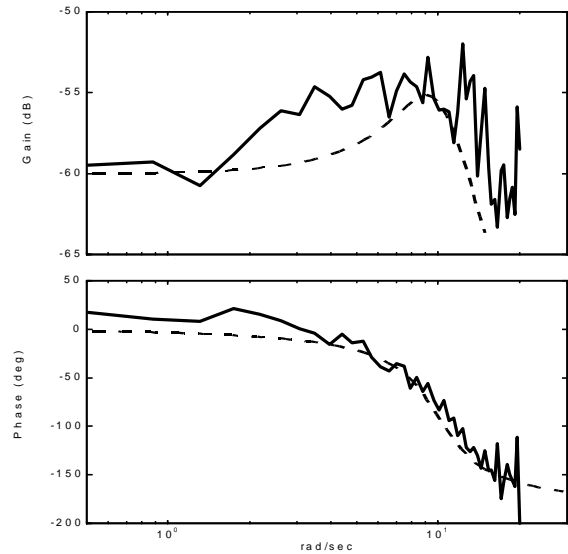


Figure 4. Elevator force to elevator deflection frequency response, actual(-) and estimated(--).

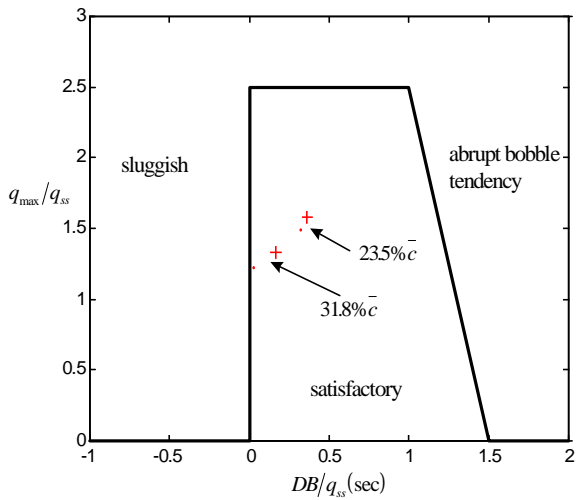


Figure 5. Dropback boundaries (after Mooij) elevator deflection to pitch rate (+) long. stick force to pitch rate (-)

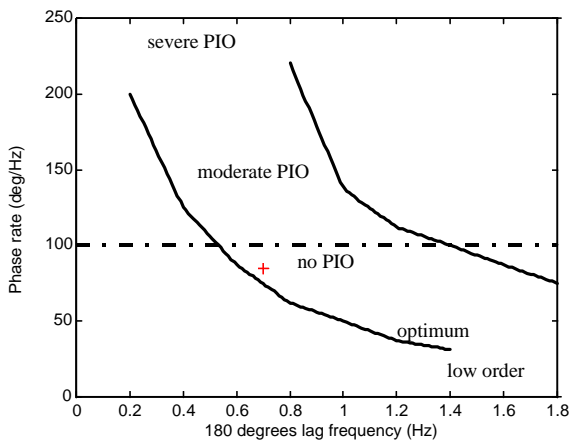


Figure 6. Phase rate boundaries long. stick force to pitch attitude, 23.5 % \bar{c} (+)

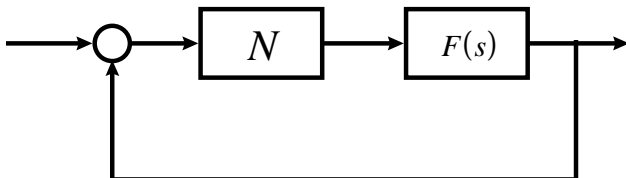


Figure 7. Closed loop system containing linear and nonlinear elements.

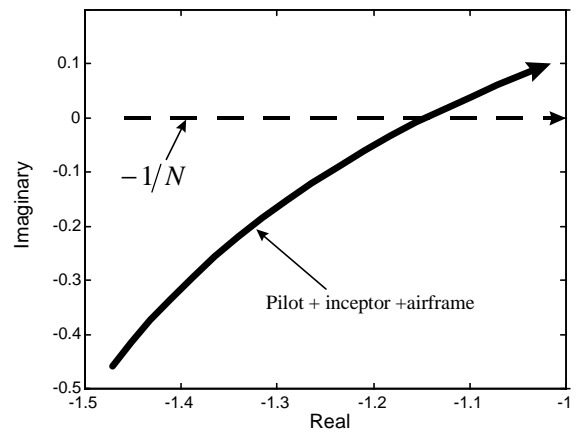


Figure 8. Nonlinear stability on the Nyquist diagram c.g. 23.5 % \bar{c}

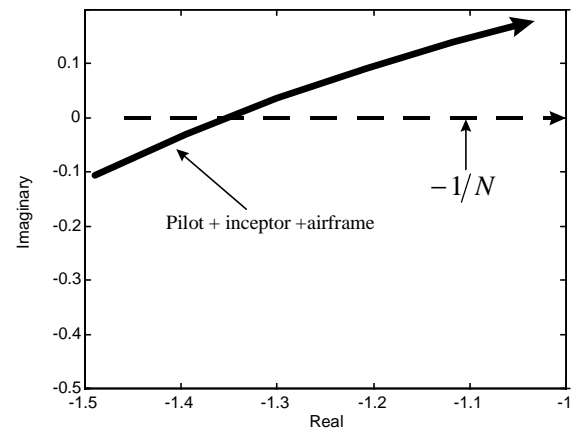


Figure 9. Nonlinear stability on the Nyquist diagram c.g. 31.8 % \bar{c}